Artificial Signal Cascades

DOI: 10.1002/anie.201310437

Nanobiomolecular Multiprotein Clusters on Electrodes for the Formation of a Switchable Cascadic Reaction Scheme**

Sven C. Feifel, Andreas Kapp, Roland Ludwig, and Fred Lisdat**

Abstract: *A supramolecular multicomponent protein architecture on electrodes is developed that allows the establishment of bidirectional electron transfer cascades based on interprotein electron exchange. The architecture is formed by embedding two different enzymes (laccase and cellobiose dehydrogenase) and a redox protein (cytochrome c) by means of carboxy-modified silica nanoparticles in a multiple layer format. The construct is designed as a switchable dual analyte detection device allowing the measurement of lactose and oxygen, respectively. As the switching force we apply the electrode potential, which ensures control of the redox state of cytochrome c. The two signal chains are operating in a non-separated matrix and are not disturbed by the other biocatalyst.*

Biochemical pathways and signal chains are characterized by an effective coupling of individual reaction steps. This results in a rather high specificity in signal transduction. Furthermore, these highly complex systems allow a switching between different reaction cascades, depending on external or internal stimuli, as for example the presence of a certain substance. With respect to redox reactions, photosynthesis and the respiratory chain are famous examples for such systems based on sequential reaction steps with high precision.[1–4] Such pathways mainly rely on the production of molecules for subsequent conversion, the use of small shuttle molecules interacting with defined components of the chain or direct reaction of protein molecules. Apparently, these efficient biological principles have been adopted for the construction of artificial signal chains.[5–7] In such a way, protein functionalities can be coupled to electrochemical detection schemes, allowing for signal generation in the presence of individual substances or certain types of molecules.[8–10] This concept has not only relevance in biosensor research,[11,12] biofuel cell development,[13,14] and logic-gate sensing schemes,[15,16] but also for the construction of biohybrid systems mimicking essential biological functions.

[*] Dr. S. C. Feifel, A. Kapp, Prof. Dr. F. Lisdat
Technical University of Applied Sciences Wildau
Biosystems Technology
Hochschulring 1, 15745 Wildau (Deutschland)
E-mail: feifel@th-wildau.de
flisdat@th-wildau.de
Dr. R. Ludwig
Food Biotechnology Laboratory
University of Natural Resources and Life Sciences
Muthgasse 18, 1190 Vienna (Austria)

[**] This work was supported by the DFG (LI706I7-1).
Supporting information for this article is available on the WWW under http://dx.doi.org/10.1002/anie.201310437.

Based on the developments in protein electrochemistry in the last decades, significant progress has been achieved in the construction of advanced bioelectronic entities. The choice is by no means limited to a monolayer arrangement of proteins on electrodes.[17,18] A diverse spectra of different approaches have been reported for multilayer formation using polyelectrolytes,[19,20] biospecific interactions,[21,22] covalent coupling,[23,24] redox polymers,[25,26] nanoparticles,[27,28] or "molecular wires".[29,30] These systems exploit sequential reactions and several electron-transfer steps. A particular group of systems make use of direct protein–protein interactions and confine their reactions to electrode surfaces. The addressed developments are based on cytochrome *c* (cyt *c*) multilayers allowing for efficient electron transfer through the entity,[31,32] as well as for an effective coupling with several biocatalysts.[33–36]

Herein we present a novel system that allows an activity switch between two enzymes co-immobilized in a supramolecular network. As switching force, we apply the electrode potential. This type of signal chain is formed by embedding two different biocatalysts, the multi-copper enzyme laccase[37] (Lac), the multi-domain enzyme cellobiose dehydrogenase[38] (CDH), and the redox protein cytochrome *c* (cyt *c*) in an artificial matrix composed of carboxy-modified silica nanoparticles (SiO_2NPs; Figure 1). With such a system, we have been able to construct a bidirectional electron transfer cascade providing the basis for dual analyte detection.

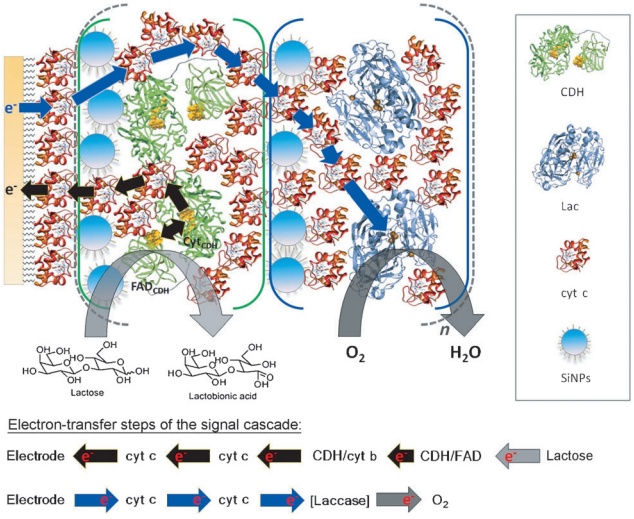

Figure 1. Representation of a $[SiO_2$NP/CDH·cyt *c*/SiO_2NP/Lac·cyt *c*$]_n$ multiprotein architecture prepared on a cyt *c* monolayer electrode. The cyt *c* monolayer is assembled on a mixed thiol layer (MU/MUA). Layer structure (n = 1, 2, 3, 4-tetralayers).

To switch on the activity of laccase, electrons have to be delivered for oxygen reduction. On the other hand, for the activation of the enzyme CDH, the electrons generated during sugar oxidation need to be collected. This role is intended to be performed by cyt *c*. Consequently by adjusting the redox state of cyt *c* in the entire supramolecular network the activity of the two different biocatalysts can be simply switched on and off. Both enzymes have been chosen since cyt *c*–enzyme interaction have been shown with the proteins in solution before.[39–41]

The entity is designed as a dual analyte measuring device in order to detect both lactose and oxygen. Thereby, we confine the CDH-cyt *c* and Lac-cyt *c* interprotein ET reaction to a surface and couple it with cyt *c* self-exchange and the direct electron transfer (DET) of cyt *c* to the transducing electrode. Non-conducting SiO_2 NPs have been modified with a carboxylic function to ensure electrostatic interactions with the proteins.

The tri-protein architecture with embedded Lac, CDH, cyt *c*, and SiO_2 NPs as scaffold is assembled on a cyt *c* monolayer by alternating incubation steps in solutions of SiO_2 NPs, cyt *c*/CDH, and cyt *c*/Lac mixtures. The monolayer electrode consists of cyt *c* adsorbed on a mixed thiol layer of mercaptoundecanoic acid (MUA) and mercaptoundecanol (MU). A representation of the modular architecture is shown in Figure 1.

The arrangement makes use of the different net charges of the proteins. As CDH and Lac possess a negative net charge and cyt *c* a positive charge at pH 7, this can be used to form precomplexes of cyt *c*/CDH and cyt *c*/Lac in a defined mixture, with an excess of cyt *c* to interact with the negative charges on the SiO_2 NP surface. The formation of the entity with cyt *c*, Lac, CDH, and SiO_2 NPs on a gold surface can be confirmed by quartz crystal microbalance (QCM) experiments, which indicate a defined binding of the components to the surface (see the Supporting Information). By definition an arrangement composed of four immobilization steps (SiO_2 NP, CDH/cyt *c*, SiO_2 NP, Lac/cyt *c*) is termed here as a tetralayer.

To ascertain the electrochemical characteristics, tri-protein electrodes [cyt *c*/SiO_2 NPs/cyt *c*·CDH/SiO_2 NPs/cyt *c*·Lac]$_{1-4}$ are studied by cyclic voltammetry (CV). In a first evaluation, only the cyt *c* molecules in the layered architectures are investigated at higher scan rates (Figure 2). The CVs show that the cyt *c* molecules in the nanobiomolecular assembly are electroactive. The amount of addressable cyt *c* correlates with the number of assembly steps, as it increases with the number of layers deposited (four tetralayers $\Gamma = 79\ \text{pmol cm}^{-2}$). The distinct increase proves the efficient electron transfer by cyt *c*–cyt *c* exchange throughout the system despite the presence of two different enzymes.

The communication of the cyt *c* molecules in the different protein stacks is only one precondition for a functional system composed of three different proteins which are arranged to exchange electrons with each other. Therefore, to examine the catalytic properties of the enzyme CDH in this triprotein entity, the electrode is exposed to a lactose containing solution and CV is performed at small scan rates ($3\ \text{mV s}^{-1}$). Here a substantial oxidation current can be observed starting from potentials around −0.05 V vs. Ag/AgCl (Figure 3). The monitored catalytic current of the system originates from lactose oxidation at CDH molecules. The reaction cascade can be described as followed: the catalytic oxidation reaction at the FAD-domain of CDH provides the electrons, which are in turn transferred to the heme-cyt *b*-domain of CDH by intraprotein ET and from there by cyt *b*–cyt *c* and cyt *c*–cyt *c* interprotein ET towards the electrode, as catalysis occurs only in the potential range of cyt *c* conversion (Figure 1). Furthermore, it has been seen in control experiments in which only cyt *c* is immobilized that no catalytic response to lactose can be observed.

To investigate the efficiency of the signal chain, the dependence of the catalytic response on the number of immobilized layers is studied. For this purpose, electrodes with different numbers of [cyt *c*/SiO_2 NPs/cyt *c*·CDH/SiO_2 NPs/cyt *c*·Lac]$_n$ tetralayers are prepared and analyzed

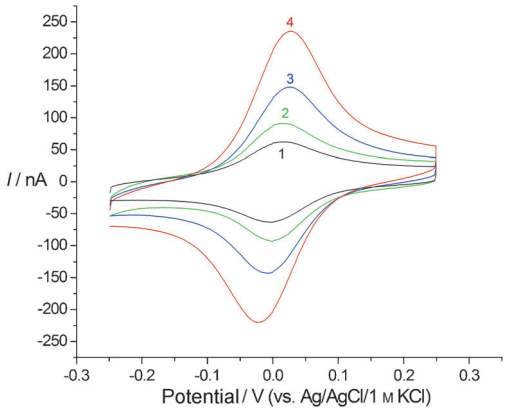

Figure 2. Cyclic voltammograms of 1–4 Au-MUA/MU-cyt *c*-[SiO_2 NPs/cyt *c*·CDH/SiO_2 NPs/cyt *c*·Lac]$_n$ tetralayer electrodes (each tetralayer contains two cyt *c* layers) measured at higher scan rates ($100\ \text{mV s}^{-1}$) in lactose-free buffer. The increase of the addressable cyt *c* is shown with increasing number of layers, compared to a monolayer electrode (pH 7, 5 mM potassium phosphate buffer).

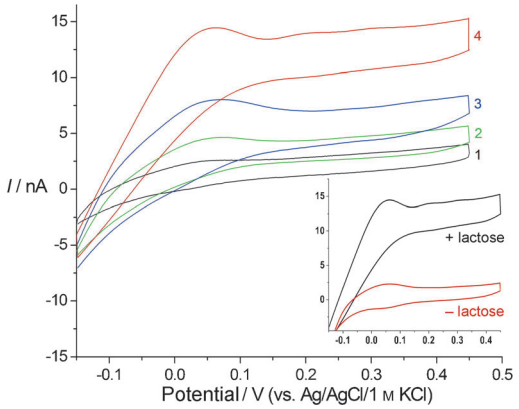

Figure 3. Cyclic voltammograms of Au-MUA/MU-cyt *c*-[SiO_2 NPs/cyt *c*·CDH/SiO_2 NPs/cyt *c*·Lac]$_{1-4}$ electrodes (tetralayers ($n = 1, 2, 3, 4$) with lactose 5 mM (scan rate $3\ \text{mV s}^{-1}$, pH 4.5, 20 mM phosphate–citrate buffer). Catalytic currents are determined for the CDH in the multilayer system. Inset: cyclic voltammogram of a four tetralayer electrode with and without lactose.

Table 1: Catalytic currents and cyt *c* concentrations in the triprotein architectures build of 1–4 tetralayers.

Dual enzyme electrodes	Number of tetralayers	Cyt *c* conc.[a] [pmol cm^{-2}]	Cat. current [nA][b] Lac[c]	CDH[d]
CDH·Lac	1	21 ± 2	−26 ± 1	4 ± 1
CDH·Lac	2	40 ± 3	−45 ± 2	6 ± 1
CDH·Lac	3	63 ± 3	−70 ± 6	9 ± 2
CDH·Lac	4	79 ± 8	−110 ± 11	15 ± 2

[a] Cyt *c* concentrations are determined by calculating the peak area in CV at 100 mV s^{-1}. [b] Catalytic currents are measured after the addition of 5 mM lactose (CDH, at positive polarization) or in air-saturated buffer (Lac, at negative polarization) at a scan rate of 3 mV s^{-1}. [c] At −200 mV. [d] At +450 mV.

by CV at pH 4.5. On basis of the recorded CV data, it can be shown that with an increased number of layers the catalytic current increases accordingly (Table 1).

About a fourfold enhancement of the catalytic current is found for a four tetralayer compared to a one tetralayer electrode. The apparent increase of the catalytic current and the amount of electroactive cyt *c* with growing number of deposited triprotein layers provides evidence for an efficient electron transfer through the architecture. It also implicates that CDH and cyt *c* molecules deposited in different stacks are in electrical contact with the electrode. This allows a cascade-like activity increase when lactose is diffusing into the multilayered system.

Although laccase has been co-immobilized in the nanobiomolecular system, the activity cannot be detected in the same potential range as applied for CDH. By switching the potential in the CV experiments to more negative values, a significant reduction current is observed, which is caused by the reduction of oxygen (Figure 4). The catalytic current results from reduction of cyt *c*, which is enhanced by subsequent oxidation by neighboring laccase molecules. Oxygen reduction near the potential of cyt *c* conversion verifies the proposed functionality of the switchable protein

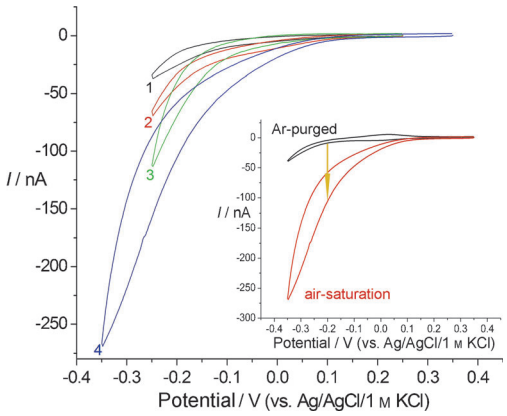

Figure 4. Cyclic voltammograms of Au-MUA/MU-cyt *c*-[SiO_2 NPs/cyt *c*·CDH/SiO_2 NPs/cyt *c*·Lac]$_{1-4}$ electrodes measured in air saturated buffer (scan rate 3 mV s^{-1}, pH 4.5, 20 mM phosphate-citrate buffer). Inset: cyclic voltammogram of a four tetralayer electrode in air-saturated and argon-purged buffer.

architecture. Thus, a second signal chain can be concluded which starts from the electrode where cyt *c* is reduced and the electrons are transferred by the cyt *c*–cyt *c* interprotein ET to the T1 center of laccase and from there to the trinuclear copper cluster at which the electrons are used for molecular O_2 reduction to produce water (Figure 1).

To gain an impression of the influence of the number of immobilized Lac layers on the catalytic reduction current, electrodes with different numbers of layers are investigated by determining the difference in the reduction current, at −200 mV in air-saturated buffer (Figure 4). From the CVs, it can be clearly seen that the reduction current increases by increasing the number of tetralayers. This means that by raising the number of catalytic sites (amount of laccase), the bioelectrocatalytic conversion of oxygen can be enhanced. This is accompanied by an increase in cytochrome *c* amount, acting as electron shuttle for both enzymes in the system (Figure 2).

To evaluate whether the protein-based signal chains can follow the concentration of the substrates, the assembly is analyzed for different lactose (for CDH) and oxygen (for Lac) concentrations (see the Supporting Information). The collected data display a linear dependence of the reduction current on the O_2 concentration (0–100% air saturation) or of the oxidation current on the lactose (0.02–1.0 mM) content in solution, respectively (3 mV s^{-1}). As the dual-enzyme system can follow the enhanced oxygen or lactose conversion at the laccase or CDH, respectively, it suggests that the overall current through the triprotein architecture is limited at least in this concentration range by the catalytic reduction (Lac) or oxidation (CDH) at the enzymes rather than by the reactions between the enzymes and cyt *c*, cyt *c*, and cyt *c* or cyt *c* and the electrode.

As already mentioned above, the enzymes and the redox protein have different functions within the dual architecture. Therefore, the relative amount of CDH or Lac and cyt *c* in each layer should have a profound effect on oxygen reduction or lactose oxidation. When the cyt *c*/CDH ratio is decreased from 20:1 to 10:1, we observe a significant decrease in the catalytic response. Therefore, although the number of recognition sites for lactose is increased (larger amount of CDH), the withdrawal of electrons from the enzyme becomes limiting and thus the activity is diminished. When high concentrations of CDH are present, the electron pathway from cyt *c* to cyt *c* seems to be disturbed. Such a behavior has also been observed for the cyt *c*/Lac ratio (< 20:1) in terms of the catalytic response.

In conclusion, we developed a layered protein architecture on electrodes allowing for two functional signal chains based on protein–protein reactions. For this purpose the enzyme CDH, Lac, and the redox protein cyt *c* are arranged by means of charged silica nanoparticles in a layer-by-layer design. Within this layered nanobiomolecular architecture, two enzymes can be connected to the electrode by cytochrome *c* in an immobilized state. As the activity of the enzymes is controlled by the delivery or withdrawal of electrons, the redox state of cyt *c* can be used for switching the activity of the biocatalysts on and off. Given that the electron transfer throughout the layered entity is feasible, laccase and cello-

biose dehydrogenase in different distances to the electrode can be addressed. The switchable reaction cascades for Lac and CDH function in an unseparated matrix without disturbing the reaction of the other participant. Cyt *c* acts as bidirectional molecular wire on the basis of interprotein electron transfer. The approach is expected to open the way for the development of multiplex biosensors, and is also a significant advance in mimicking of biological electron-transfer cascades.

Received: December 2, 2013
Revised: January 17, 2014
Published online: April 11, 2014

Keywords: artificial signal chains · cellobiose dehydrogenase · interprotein electron transfer · laccase · nanoparticles

[1] J. F. Turrens, *J. Physiol.* **2003**, *552*, 335.
[2] A. N. Glazer, A. Melis, *Annu. Rev. Plant Physiol. Plant Mol. Biol.* **1987**, *38*, 11.
[3] G. W. Brudvig, R. H. Crabtree, *Proc. Natl. Acad. Sci. USA* **1986**, *83*, 4586.
[4] P. S. Brookes, A. L. Levonen, S. Shiva, P. Sarti, V. M. Darley-Usmar, *Free Radicals Biol. Med.* **2002**, *33*, 755.
[5] I. Willner, E. Katz, *Angew. Chem.* **2000**, *112*, 1230; *Angew. Chem. Int. Ed.* **2000**, *39*, 1180.
[6] T. Ikeda, K. Kano, *J. Biosci. Bioeng.* **2001**, *92*, 9.
[7] C. Bourdillon, C. Demaille, J. Moiroux, J.-M. Saveant, *Acc. Chem. Res.* **1996**, *29*, 529.
[8] E. E. Ferapontova, T. Ruzgas, L. Stoica, A. Christenson, J. Tkac, A. I. Yaropolov, L. Gorton, *Perspect. Bioanal.*, *Vol. 1*, Elsevier, Dordrecht, **2005**, p. 517.
[9] J. F. Rusling, *Acc. Chem. Res.* **1998**, *31*, 363.
[10] C. J. McNeil, D. Athey, W. O. Ho, *Biosens. Bioelectron.* **1995**, *10*, 75.
[11] D. Grieshaber, R. MacKenzie, J. Vörös, E. Reimhult, *Sensors* **2008**, *8*, 1400.
[12] F. Lisdat, R. Dronov, H. Möhwald, F. W. Scheller, D. G. Kurth, *Chem. Commun.* **2009**, 274.
[13] D. P. Hickey, F. Giroud, D. W. Schmidtke, D. T. Glatzhofer, S. D. Minteer, *ACS Catal.* **2013**, *3*, 2729.
[14] M. J. Moehlenbrock, T. K. Toby, L. N. Pelster, S. D. Minteer, *ChemCatChem* **2011**, *3*, 561.
[15] O. Zavalov, V. Bocharova, V. Privman, E. Katz, *J. Phys. Chem. B* **2012**, *116*, 9683.
[16] J. Wang, E. Katz, *Anal. Bioanal. Chem.* **2010**, *398*, 1591.
[17] I. Taniguchi, S. Yoshimoto, K. Nishiyama, *Chem. Lett.* **1997**, 353.
[18] B. Ge, F. Lisdat, *Anal. Chim. Acta* **2002**, *454*, 53.
[19] N. Jessel, F. Atalar, P. Lavalle, J. Mutterer, G. Decher, P. Schaaf, J. C. Voegel, J. Ogier, *Adv. Mater.* **2003**, *15*, 692.
[20] F. Mizutani, Y. Sato, S. Yabuki, Y. Hirata, *Chem. Lett.* **1996**, *25*, 251.
[21] C. Bourdillon, C. Demaille, J. Moiroux, J.-M. Saveant, *J. Am. Chem. Soc.* **1994**, *116*, 10328.
[22] J. Anzai, H. Takeshita, Y. Kobayashi, T. Osa, T. Hoshi, *Anal. Chem.* **1998**, *70*, 811.
[23] I. Willner, A. Riklin, B. Shoham, D. Rivenzon, E. Katz, *Adv. Mater.* **1993**, *5*, 912.
[24] W. Jin, F. Bier, U. Wollenberger, F. W. Scheller, *Biosens. Bioelectron.* **1995**, *10*, 823.
[25] C. Demaille, J. Moiroux, *J. Phys. Chem. B* **1999**, *103*, 9903.
[26] S. F. Hou, K. S. Yang, H. Q. Fang, H. Y. Chen, *Talanta* **1998**, *47*, 561.
[27] H. Y. Liu, J. F. Rusling, N. F. Hu, *Langmuir* **2004**, *20*, 10700.
[28] Y. Zhang, H. Lu, N. Hu, *J. Phys. Chem. B* **2005**, *109*, 10464.
[29] I. Willner, V. Heleg-Shabtai, R. Blonder, E. Katz, G. Tao, *J. Am. Chem. Soc.* **1996**, *118*, 10321.
[30] F. Patolsky, Y. Weizmann, I. Willner, *Angew. Chem.* **2004**, *116*, 2165; *Angew. Chem. Int. Ed.* **2004**, *43*, 2113.
[31] M. K. Beissenhirtz, F. W. Scheller, W. F. M. Stöcklein, D. G. Kurth, H. Möhwald, F. Lisdat, *Angew. Chem.* **2004**, *116*, 4457; *Angew. Chem. Int. Ed.* **2004**, *43*, 4357.
[32] S. C. Feifel, F. Lisdat, *J. Nanobiotechnol.* **2011**, *9*, 59.
[33] R. Dronov, D. G. Kurth, H. Möhwald, F. W. Scheller, F. Lisdat, *Angew. Chem.* **2008**, *120*, 3042; *Angew. Chem. Int. Ed.* **2008**, *47*, 3000.
[34] S. C. Feifel, R. Ludwig, L. Gorton, F. Lisdat, *Langmuir* **2012**, *28*, 9189.
[35] R. Spricigo, R. Dronov, F. Lisdat, S. Leimkühler, F. W. Scheller, U. Wollenberger, *Anal. Bioanal. Chem.* **2009**, *393*, 225.
[36] F. Wegerich, P. Turano, M. Allegrozzi, H. Möhwald, F. Lisdat, *Langmuir* **2011**, *27*, 4202.
[37] S. Shleev, J. Tkac, A. Christenson, T. Ruzgas, A. I. Yaropolov, J. W. Whittaker, L. Gorton, *Biosens. Bioelectron.* **2005**, *20*, 2517.
[38] L. Stoica, T. Ruzgas, R. Ludwig, D. Haltrich, L. Gorton, *Langmuir* **2006**, *22*, 10801.
[39] V. Fridman, U. Wollenberger, V. Bogdanovskaya, F. Lisdat, T. Ruzgas, A. Lindgren, L. Gorton, F. W. Scheller, *Biochem. Soc. Trans.* **2000**, *28*, 63.
[40] M. J. Tarlov, E. F. Bowden, *J. Am. Chem. Soc.* **1991**, *113*, 1847.
[41] W. Jin, U. Wollenberger, F. Bier, A. Makover, F. W. Scheller, *Bioelectrochem. Bioenerg.* **1996**, *39*, 221.

